

Relativistic precession and spin dynamics of an elliptic Rydberg wave packet

P Rozmej[†], M Turek[‡], R Arvieu[♣], and I S Averbukh[♣] ¶

[†] Institute of Physics, University of Zielona Góra, 65-246 Zielona Góra, Poland
p.rozmej@im.pz.zgora.pl

[‡] Institute of Physics, Maria Curie-Skłodowska University, 20-031 Lublin, Poland
mturek@kft.umcs.lublin.pl

[♣] Institut des Sciences Nucléaires, F 38026 Grenoble Cedex, France
arvieu@in2p3.fr

[♣] The Weizmann Institute of Science 76100 Rehovot, Israel
ilya.averbukh@weizmann.ac.il

Abstract. Time evolution of wave packets built from the eigenstates of the Dirac equation for a hydrogenic system is considered. We investigate the space and spin motion of wave packets which, in the non-relativistic limit, are stationary states with a probability density distributed uniformly along the classical, elliptical orbit (elliptic WP). We show that the precession of such a WP, due to relativistic corrections to the energy eigenvalues, is strongly correlated with the spin motion. We show also that the motion is universal for all hydrogenic systems with an arbitrary value of the atomic number Z .

PACS numbers: 03.65.P, 03.65, 03.65.S

The detailed study of the time evolution of quantum wave packets (WPs) in simple atomic or molecular systems has been the object of growing attention for more than ten years [1]. Most of the previous theoretical studies were done in non-relativistic framework. In the field of relativistic quantum mechanics most of the efforts have been focused on the problem of the interaction between the atoms and a mixture of static fields with, most of the time, intense laser fields [2–11]. Under these conditions the use of a relativistic theory is fully justified since the external field is then able to bring considerable energy to the WP. For isolated atoms, however, the use of relativistic dynamics is more questionable, if the WP is followed or observed only during a short period of time. In ref. [12] relativistic wave packets, corresponding to circular orbits, have been constructed for hydrogenic atoms with a large Z , and propagated over time according to the Dirac equation. Particular attention was paid to the spin collapse event, *i.e.* to the maximum entanglement, in the course of time, of the spin degree of freedom with the spatial ones. This phenomenon was first shown to take place for a WP in a harmonic oscillator with a spin-orbit force [13], where it is periodic. For this reason it has been called the *spin-orbit pendulum*. In the Dirac equation with a Coulomb

¶ Research supported by KBN grants No. 5 P03B 010 20 and 5 P03B 104 21

potential, it is produced by the built-in spin-orbit force and it is not periodic. The time scale where this effect can manifest itself was discussed in ref. [12], as a function of the charge Z of the atom and the average principal quantum number N of the WP. This phenomenon is expected to take place on a longer time scale like the other time dependent quantum effects of spreading and of fractional revivals [14]. We intend below to complement this work by studying the possible relativistic precession of elliptic WPs and by comparing this precession to the spin motion. A preliminary version of the present work was already presented at the ECAMP VII conference [15].

There are two possible ways to build up a WP 'on top of a classical elliptic orbit' in non-relativistic mechanics. One of them is by kicking properly a well designed WP, for example a Gaussian WP, that is then evolved in time by the free Hamiltonian until it spreads above an average classical ellipsis. This method is not very easy to apply and its main inconvenience is to produce an internal motion within the ellipsis that is able to blur the precession. Therefore, we have preferred a second method, much simpler and even more elegant, which consists of using the coherent WPs of ref. [16], which are stationary states of the non-relativistic Coulomb problem. The space probability density of these states was indeed shown to be highly concentrated around a classical Bohr-Sommerfeld ellipsis. If these states can be adapted to relativistic dynamics their time evolution will doubtlessly be due to relativistic effects, *i.e.* due to the fine structure that will act as a perturbation. Let us first show how to adapt these states to a relativistic theory. We want the spatial part of the large components of the new WP to tend (in the non-relativistic limit) toward the state $|n\gamma\rangle$ of [16] which is defined as

$$|n\gamma\rangle = \sum_{l,m} (-1)^{(l+m)/2} \frac{2^{n-l-1}(n-1)!}{[(l-m)/2]![(l+m)/2]!} \left[\frac{(l+m)!(l-m)!(2l+1)}{(n-l-1)!(n+l)!} \right]^{1/2} \\ \times \left(\sin \frac{\gamma}{2} \right)^{n-m-1} \left(\cos \frac{\gamma}{2} \right)^{n+m-1} |n, l, m\rangle = \sum_{lm} w_{lm}^{(n)} |n, l, m\rangle. \quad (1)$$

The probability density $\langle n\gamma|n\gamma\rangle$ is fairly localized onto a Bohr orbit with eccentricity $\epsilon = \sin \gamma$ and the average angular momentum is

$$l_{av} = (n-1) \cos \gamma, \quad (2)$$

where n is the principal quantum number of the orbitals $|n, l, m\rangle$ which are admixed in (1). The sum contains $n(n+1)/2$ values of m with $l+m$ even. The contribution of states with $m < l$ decreases very rapidly with m (more than one order of magnitude for each 2 units of m as shown in fig. 1). The dominant weights are those with $m = l$ and their distribution is nearly Gaussian. The relative contribution of states with $m < l$ increases, however, for larger values of the eccentricity parameter ϵ . The larger admixture of these states causes much faster daphasing of the WP. Therefore for illustration of typical precession phenomena he have chosen the case $\epsilon = 0.4$.

In order to study the entanglement of the spin degrees of freedom with the orbital ones, it is natural in a non-relativistic theory to start from a product state of an arbitrary

spinor $\begin{pmatrix} a \\ b \end{pmatrix}$ with the state $|n\gamma\rangle$.

$$|\Psi_{nr}\rangle = |n\gamma\rangle \begin{pmatrix} a \\ b \end{pmatrix} = \sum_{lm} w_{lm}^{(n)} |n, l, m\rangle \begin{pmatrix} a \\ b \end{pmatrix}. \quad (3)$$

It may be expanded in eigenstates of total angular momentum $|n, l, j = l + s, m_j\rangle$ with $m_j = m + 1/2$ or $m - 1/2$ and $s = +1/2$ or $-1/2$.

$$|\Psi_{nr}\rangle = \sum_{lm} w_{lm}^{(n)} \left\{ a \left(\sqrt{\frac{l+1+m}{2l+1}} |n, l, j_>, m+1/2\rangle - \sqrt{\frac{l-m}{2l+1}} |n, l, j_<, m+1/2\rangle \right) \right. \\ \left. + b \left(\sqrt{\frac{l+1-m}{2l+1}} |n, l, j_>, m-1/2\rangle + \sqrt{\frac{l+m}{2l+1}} |n, l, j_<, m-1/2\rangle \right) \right\}. \quad (4)$$

In a similar way as in ref. [12], for a circular WP, the state (4) is transformed into a four component relativistic state Ψ_r by replacing in (4) the non-relativistic states $|n, l, j, m_j\rangle$ by the eigenstates of the Dirac equation with the same quantum numbers. In this manner the WP gets small components in the most natural way. The radial parts of the large and of the small components are taken obviously as different ones. The probability density of the relativistic WP built in this way is represented in fig. 2.

The time evolution of the WP is produced by introducing the phase factors $\exp(-iE_l^+ t)$ and $\exp(-iE_l^- t)$ as coefficients of states with $j = l + 1/2$ and $j = l - 1/2$ with their corresponding eigenvalues. The four components $c_i(t)$ $i = 1, \dots, 4$ of the WP at time t are given in the Appendix A with Ψ_r defined as

$$|\Psi_r(t)\rangle = \begin{pmatrix} |c_1(t)\rangle \\ |c_2(t)\rangle \\ |c_3(t)\rangle \\ |c_4(t)\rangle \end{pmatrix}. \quad (5)$$

It should be stressed that Ψ_r for $t = 0$ is not any more a product state of the form of eq. (3) due to the built-in entanglement contained in the solutions of the Dirac equation. However, since the small components of Ψ_r are indeed very small, this defect has no important effect on the magnitude of the initial spin. Since the spin-orbit coupling effect, *i.e.* spin-orbit pendulum [13], manifests itself more efficiently if s and l are perpendicular to each other, we choose for our discussion:

$$a = b = \frac{1}{\sqrt{2}} \quad i.e. \quad \langle s_x \rangle_{nr} = \frac{1}{2}. \quad (6)$$

Precession of quantum elliptical states in the Coulomb field has already been considered in ref. [17], starting also from the same coherent state as done here. However, the precession was studied only in non-relativistic quantum dynamics as a perturbation effect and no treatment of the spin was attempted.

Let us finally discuss the time units relevant to our problem. To the lowest order in terms of the fine structure constant, the energy of an eigenstate $|n, l, j = l + s\rangle$ of the Dirac equation can be written (in a.u.) for a hydrogenic atom of charge Z as

$$E_{nlj} = \bar{E}_n - \frac{1}{2} \frac{Z^4 \alpha^2}{n^3 (l + s + 1/2)} \quad (7)$$

with $s = +1/2$ or $-1/2$. The constant energy \bar{E}_n produces no effect on WP, since it depends only on n . Let us define an average time unit T_p (p for precession):

$$T_p = \frac{2\pi}{\langle \frac{dE_{nlj}}{dt} \rangle} \quad (8)$$

$$= \frac{4\pi n^3}{Z^4 \alpha^2} \langle (l + s + \frac{1}{2})^2 \rangle \approx \frac{4\pi n^3 l_{av}^2}{Z^4 \alpha^2} \quad (9)$$

$$= \frac{2 l_{av}^2 T_K}{(Z\alpha)^2} . \quad (10)$$

Brackets $\langle \rangle$ in (8)-(9) denote average values, l_{av} is given by (2). For $n = 50$, $\epsilon = 0.4$ precession time T_p ranges from $1.96 \cdot 10^{-11}$ s for $Z = 92$ to $1.4 \cdot 10^{-3}$ s for $Z = 1$. T_K in (10) denotes the Kepler period.

It is necessary to compare T_p to the radiative lifetime $T_{n,l}^{\text{rad}}$ of hydrogenic levels. We will use the estimation of $T_{n,l}^{\text{rad}}$ for a single n, l state given in [18]. In atomic units it is

$$T_{n,l}^{\text{rad}} = \frac{3}{2\alpha^3 Z^4} n^3 \left(l + \frac{1}{2} \right)^2 , \quad (11)$$

which was found to agree within 10% with experimental data. One obtains the universal ratio:

$$\frac{T_p}{T_{n,l}^{\text{rad}}} = \frac{8\pi\alpha}{3} \approx 0.061 \quad (12)$$

which guarantees that the precession of the wave packet takes place long enough time before even a single photon is emitted. The occurrence of α in this ratio is understandable, since T_p is a classical-like quantity, while $T_{n,l}^{\text{rad}}$ is proportional to $1/\hbar$, because it can be expressed as a ratio of a typical energy of the emitted photon to the classical radiation rate corresponding to the orbital motion.

When $t = T_p$ the linear terms in the expansion of E_{nlj} in the power of l contribute on the average to 2π in the exponential factors and the WP is expected to restore. However the terms of the higher order dephase differently the various partial waves, and this leads to a spreading of the WP near the initial shape [14]. See the discussion on the magnitude of these terms in Appendix B. Expression (10) or (11) (with the Kepler period $T_K = 2\pi n^3/Z^2$) is also recognized as the classical precession time in the relativistic Coulomb problem [19].

Let us note that dE_{nlj}/dl is also (to the first order) the energy difference between two spin-orbit partners. Therefore the precession time can also be interpreted as the recurrence time of the spin. Hence we should observe a strong correlation between the spatial motion of the density: the precession, and the spin motion.

Let us discuss now the dynamics dependence on the atomic number, Z . Formula (9) suggests that the relativistic effects under consideration in this article, depend crucially on Z . For sure the highest possible Z are indeed required to lower T_p as much as possible. It is interesting to stress nevertheless, that within a very good approximation, a scaling of Z is possible which leads to the universal behaviour of the wave packet (1).

First of all since E , approximated by eq. (7), scales as Z^4 , *i.e.* as T_p^{-1} , the variable Z disappears from Et if we use the reduced time t/T_p . The autocorrelation function (A.20) which is expressed only in terms of Et is the simplest quantity which has a universal behaviour, provided the same n and ϵ are used for all values of Z .

The other quantities, like the probability density and the the spin expectation values depend on the radial wave functions and radial integrals. In a non-relativistic theory scaling of the radial wave function is elementary, it is obtained by dividing the radial wave function by $Z^{3/2}$ and multiplying the radial variable by Z . This is an exact property. The ratio small/large components of the relativistic solutions scale as $\sqrt{(1-E)/(1+E)}$, *i.e.* roughly like Z^2 and the radial wave functions depend also in a more complicated manner on Z . Nevertheless, on the whole as seen in fig. 5 below, the small components contribute a very small part of the probability density even for $Z = 92$ (see also fig. 1 of ref. [12]). The scaling of the probability density is therefore entirely governed by the large components *i.e.* by the non-relativistic theory.

In a similar way we have checked that the radial integrals which contribute to the spin expectation values have the same properties: the integrals G_+ , G_- , and G_{+-} are equal to 1, within less than 10^{-5} and the other F_+ , $F_- \dots$ contribute in a very small manner, also of the order of 10^{-5} .

Therefore, the universal behaviour of the wave packet is justified and except for fig. 2 no value of Z is given. For longer times, the energy factors omitted in eq. (7) which involve higher powers of Z , play a role and produce a genuine Z dependence. Those effects will not be discussed here.

The probability density of the wave packet with $n = 50$, $\epsilon = 0.4$ and $a = b = 1/\sqrt{2}$, with $Z = 92$, is shown for a set of times up to $t = T_p$ in fig. 3 and fig. 4. The part of the density coming from the small components, shown in fig. 5, is also concentrated on top of an ellipsis but its magnitude is a thousands times smaller than the total density. For $t < T_p/4$ the density precesses as described classically with a small dispersion. However the spreading takes place very rapidly for larger t and is quite extended for $t = T_p$.

The precession of the ellipsis, the recurrence and spreading can be seen in a more condensed manner in the autocorrelation function represented in fig. 6 for three different spin preparations (spin up, spin down and $a = b = 1/\sqrt{2}$). For small t/T_p the WP becomes almost orthogonal to its initial parent, for $t = T_p$ a recurrence occurs but the overlap is only 0.7. Another peak occurs at $t = 2T_p$ but higher frequencies become important and spread the recurrence. For $t > 3T_p$ these higher frequencies play a dominant role. An example of an approximate revival for $t = 22.6 T_p$ is displayed in fig. 7. Fractional revivals [14] can also be seen to some extent. Two examples of 1/3 and 1/2 revivals are presented in fig. 8.

The rough independence of the autocorrelation function on the spin preparation requires some explanation. We can approximate this function by

$$\langle \Psi_r(0) | \Psi_r(t) \rangle \approx a^2 \sum_l w_{ll}^2 \exp(-iE_l^+ t) + b^2 \sum_l w_{ll}^2 \exp(-iE_l^- t), \quad (13)$$

where we have neglected the terms with very small weights $w_{l,m \neq l}^2$. The contribution of the two sums above is almost the same because w_{ll} has a smooth variation with l on the one hand, and because of the exact equality $E_l^- = E_{l-1}^+$ on the other hand.

Finally the time evolution of the spin averages is presented in fig. 9. This figure exhibits what we can call the relativistic spin-orbit pendulum. Although the wave packet is not prepared initially in a pure state of spin, the impurity is very small (for $a = b = 1/\sqrt{2}$ one has $\langle \sigma_x \rangle \approx 0.9997$). As time goes on the spin stays very nearly in the Oxy plane and rotates around Oz with period T_p . Its magnitude slowly decreases, however, and for $5 < t/T_p < 10$ the spin is almost totally entangled with the orbital motion, since the average of its three projections are almost zero. During a period of time that last for about $5T_p$ the angular momentum of the spin is transferred to the orbital motion and therefore the mean trajectory is not planar anymore [13]. Since the orbital angular momentum of $40\hbar$ is much higher than $\hbar/2$ this geometrical effect can hardly be represented graphically. From $t \approx 15T_p$ a revival of spin occurs. The spin rotates and increases its magnitude at the same time. This event stays even longer than initially. However the recurrence is only partial.

In conclusion we can say, that for not too long time, the precession and spin motion of the WPs are fairly well described by the following approximation: non-relativistic wave functions of the form (3) and relativistic energy eigenvalues. From this point of view the full, computationally very demanding, relativistic approach is unnecessary. However, this conclusion may be formulated not a priori but only a posteriori.

We would like to stress the richness of the dynamics just described. Indeed, in addition to the relativistic precession of the ellipsis we have obtained for longer times its fractional revivals. During the evolution the spin of the electron is entangled with its orbital motion to various degrees. All this agree completely with previous results [14] and [13]. However, it was obtained here in a full relativistic calculation. Since we have been able to scale the atomic number Z we have given a universal behaviour to our WP. It is, however, clear that this scaling is destroyed in real atoms in a more realistic theory which would take into account quantum defects. Their inclusion would also distort the dynamics, for example it would change the precession time, in a way that is out of reach of our simple theory. As far as purely relativistic effects are concerned, like the importance of the small components or the zitterbewegung, we have found them negligible in the Coulomb problem, in contrast to the Dirac oscillator [20] in which they play a major role.

Acknowledgments

The authors would like to express their gratitude to the two referees who attracted their attention to the interplay between relativistic precession and radiative processes (eq. (12)) in the Coulomb problem. I.S. Averbukh thanks also C.R. Stroud, Jr. for useful discussions.

Appendix A. Details of the calculations

Replacing a non-relativistic wave function in (4) by the eigenstates of the Dirac equation, one obtains for $\Psi_r(t)$:

$$\begin{aligned} \Psi_r(t) = \sum_{lm} w_{lm}^{(n)} & \left\{ a \sqrt{\frac{l+1+m}{2l+1}} \begin{pmatrix} ig_{n'_+} \Omega_{l,j>,m+1/2} \\ -f_{n'_+} \Omega_{l+1,j>,m+1/2} \end{pmatrix} \exp(-iE_l^+ t) \right. \\ & + a \sqrt{\frac{l-m}{2l+1}} \begin{pmatrix} ig_{n'_-} \Omega_{l,j<,m+1/2} \\ -f_{n'_-} \Omega_{l-1,j<,m+1/2} \end{pmatrix} \exp(-iE_l^- t) \\ & + b \sqrt{\frac{l+1-m}{2l+1}} \begin{pmatrix} ig_{n'_+} \Omega_{l,j>,m-1/2} \\ -f_{n'_+} \Omega_{l+1,j>,m-1/2} \end{pmatrix} \exp(-iE_l^+ t) \\ & \left. - b \sqrt{\frac{l+m}{2l+1}} \begin{pmatrix} ig_{n'_-} \Omega_{l,j<,m-1/2} \\ -f_{n'_-} \Omega_{l-1,j<,m-1/2} \end{pmatrix} \exp(-iE_l^- t) \right\}. \end{aligned} \quad (\text{A.1})$$

We have used the notations of [12]: $g(r)$ and $f(r)$ are the radial parts of the large and small components associated with the quantum numbers $n' = n - (j + 1/2)$. These functions are multiplied by the spherical tensors Ω_{l,j,m_j} which are defined by eq. 4a and 4b of [12]. The energy of the spin orbit partners of a given value of l is denoted by E_l^+ if $j = l + 1/2$ and E_l^- if $j = l - 1/2$, respectively.

For numerical calculations it is convenient to rewrite components of (A.1) in the following form:

$$\begin{aligned} |c_1(t)\rangle = i \sum_l & \left\{ g_{n'_+} \exp(-iE_l^+ t) \sum_m w_{lm}^{(n)} \left(a \frac{l+1+m}{2l+1} |l, m\rangle \right. \right. \\ & \left. \left. + b \frac{\sqrt{(l+1-m)(l+m)}}{2l+1} |l, m-1\rangle \right) \right. \\ & + g_{n'_-} \exp(-iE_l^- t) \sum_m w_{lm}^{(n)} \left(a \frac{l-m}{2l+1} |l, m\rangle \right. \\ & \left. \left. - b \frac{\sqrt{(l+1-m)(l+m)}}{2l+1} |l, m-1\rangle \right) \right\}, \end{aligned} \quad (\text{A.2})$$

$$\begin{aligned} |c_2(t)\rangle = i \sum_l & \left\{ g_{n'_+} \exp(-iE_l^+ t) \sum_m w_{lm}^{(n)} \left(b \frac{l+1-m}{2l+1} |l, m\rangle \right. \right. \\ & \left. \left. + a \frac{\sqrt{(l+1+m)(l-m)}}{2l+1} |l, m+1\rangle \right) \right. \\ & \left. + g_{n'_-} \exp(-iE_l^- t) \sum_m w_{lm}^{(n)} \left(b \frac{l+m}{2l+1} |l, m\rangle \right. \right. \\ & \left. \left. - a \frac{\sqrt{(l+1+m)(l-m)}}{2l+1} |l, m+1\rangle \right) \right\}, \end{aligned} \quad (\text{A.3})$$

$$\begin{aligned}
& + g_{n'_-} \exp(-iE_l^- t) \sum_m w_{lm}^{(n)} \left(b \frac{l+m}{2l+1} |l, m\rangle \right. \\
& \quad \left. - a \frac{\sqrt{(l+1+m)(l-m)}}{2l+1} |l, m+1\rangle \right) \Bigg\} , \\
|c_3(t)\rangle = \sum_l \Bigg\{ & f_{n'_+} \exp(-iE_l^+ t) \sum_m w_{lm}^{(n)} \left(a \sqrt{\frac{(l+1+m)(l+1-m)}{(2l+1)(2l+3)}} |l+1, m\rangle \right. \\
& \quad \left. + b \sqrt{\frac{(l+1-m)(l+2-m)}{(2l+1)(2l+3)}} |l+1, m-1\rangle \right) \\
& + f_{n'_-} \exp(-iE_l^- t) \sum_m w_{lm}^{(n)} \left(a \sqrt{\frac{(l+m)(l-m)}{(2l+1)(2l-1)}} |l-1, m\rangle \right. \\
& \quad \left. - b \sqrt{\frac{(l+m)(l-1+m)}{(2l+1)(2l-1)}} |l-1, m-1\rangle \right) \Bigg\} , \tag{A.4}
\end{aligned}$$

$$\begin{aligned}
|c_4(t)\rangle = \sum_l \Bigg\{ & f_{n'_+} \exp(-iE_l^+ t) \sum_m w_{lm}^{(n)} \left(-b \sqrt{\frac{(l+1+m)(l+1-m)}{(2l+1)(2l+3)}} |l+1, m\rangle \right. \\
& \quad \left. - a \sqrt{\frac{(l+1+m)(l+2+m)}{(2l+1)(2l+3)}} |l+1, m+1\rangle \right) \\
& + f_{n'_-} \exp(-iE_l^- t) \sum_m w_{lm}^{(n)} \left(-b \sqrt{\frac{(l+m)(l-m)}{(2l+1)(2l-1)}} |l-1, m\rangle \right. \\
& \quad \left. + a \sqrt{\frac{(l-m)(l-1-m)}{(2l+1)(2l-1)}} |l-1, m+1\rangle \right) \Bigg\} . \tag{A.5}
\end{aligned}$$

Using the explicit form of the WP, one obtains for the average values of the spin operators:

$$\begin{aligned}
\langle \sigma_x \rangle_t = 2ab \sum_{lm} \Bigg\{ & w_{lm}^2 \left[G_+ \frac{(l+1)^2 - m^2}{(2l+1)^2} + G_- \frac{l^2 - m^2}{(2l+1)^2} - F_+ \frac{(l+1)^2 - m^2}{(2l+1)(2l+3)} \right. \\
& \quad \left. - F_- \frac{l^2 - m^2}{(2l+1)(2l-1)} + 2G_{+-} \frac{l(l+1) + m^2}{(2l+1)^2} \cos(\omega_l t) \right] \\
& + w_{l,m} w_{l-2,m-2} \left[F_{-+} \sqrt{\frac{(l+m)(l-1+m)(l-2+m)(l-3+m)}{(2l-1)^2(2l+1)(2l+3)}} \cos(\omega_l'' t) \right] \\
& + w_{l,m} w_{l,m-2} \frac{\sqrt{(l+m)(l-1+m)}}{(2l+1)} \\
& \quad \times \left[\frac{\sqrt{(l+1-m)(l+2-m)}}{(2l+1)} [G_+ + G_- - 2G_{-+} \cos(\omega_l t)] \right] \tag{A.6}
\end{aligned}$$

$$\begin{aligned}
& \left. -\frac{\sqrt{(l+2-m)(l-3-m)}}{(2l-1)}F_- - \frac{\sqrt{(l+2-m)(l+1-m)}}{(2l+3)}F_+ \right] \\
& -w_{l,m}w_{l-2,m} \left[2F_{-+} \sqrt{\frac{(l^2-m^2)((l-1)^2-m^2)}{(2l-1)^2(2l+1)(2l-3)}} \cos(\omega_l''t) \right] \\
& +w_{l,m}w_{l+2,m-2} \left[F'_{-+} \sqrt{\frac{(l+1-m)(l+2-m)(l+3-m)(l+4-m)}{(2l+1)(2l+3)^2(2l+5)}} \cos(\omega_l't) \right] \Bigg\}, \\
\langle \sigma_y \rangle_t = 2ab \sum_{lm} & \left\{ w_{l,m}^2 \left[\frac{2m}{2l+1} G_{+-} \sin(\omega_l t) \right] \right. \\
& -w_{l,m}w_{l-2,m-2} \left[F_{-+} \sqrt{\frac{(l+m)(l-1+m)(l-2+m)(l-3+m)}{(2l-1)^2(2l+1)(2l+3)}} \sin(\omega_l''t) \right] \\
& +w_{l,m}w_{l-2,m} \left[2F_{-+} \sqrt{\frac{(l^2-m^2)((l-1)^2-m^2)}{(2l-1)^2(2l+1)(2l-3)}} \sin(\omega_l''t) \right] \\
& \left. -w_{l,m}w_{l+2,m-2} \left[F'_{-+} \sqrt{\frac{(l+1+m)(l+2-m)(l+3-m)(l+4-m)}{(2l-1)(2l+3)^2(2l+5)}} \sin(\omega_l't) \right] \right\}, \tag{A.7}
\end{aligned}$$

and

$$\begin{aligned}
\langle \sigma_z \rangle_t = \sum_{lm} & \left\{ w_{l,m}^2 \left[a^2 \frac{2m+1}{2l+1} \left(G_+ \frac{l+1+m}{2l+1} - G_- \frac{l-m}{2l+1} - F_+ \frac{l+1+m}{2l+3} + F_- \frac{l-m}{2l-1} \right) \right. \right. \\
& + b^2 \frac{2m-1}{2l+1} \left(G_+ \frac{l+1-m}{2l+1} - G_- \frac{l+m}{2l+1} - F_+ \frac{l+1-m}{2l+3} + F_- \frac{l+m}{2l-1} \right) \\
& \left. + 4G_{+-} \cos(\omega_l t) \left(a^2 \frac{(l-m)(l+1+m)}{(2l+1)^2} - b^2 \frac{(l+m)(l+1-m)}{(2l+1)^2} \right) \right] \\
& \left. + 4(a^2 - b^2) w_{l,m}w_{l+2,m} F'_{-+} \sqrt{\frac{((l+1)^2-m^2)((l+2)^2-m^2)}{(2l+1)(2l+3)^2(2l+5)}} \cos(\omega_l't) \right\} \tag{A.8}
\end{aligned}$$

In the above formulas, the following notations have been introduced:

$$\omega_l = (E_l^+ - E_l^-), \tag{A.9}$$

$$\omega_l' = (E_{l+2}^- - E_l^+), \tag{A.10}$$

$$\omega_l'' = (E_l^- - E_{l-2}^+) \tag{A.11}$$

Note that $\omega_l' = \omega_{l+2}''$. Radial integrals are denoted as follows:

$$G_+ = \int_0^\infty (g_l^+(r))^2 r^2 dr, \tag{A.12}$$

$$G_- = \int_0^\infty (g_l^-(r))^2 r^2 dr, \tag{A.13}$$

$$F_+ = \int_0^\infty (f_l^+(r))^2 r^2 dr, \tag{A.14}$$

$$F_- = \int_0^\infty (f_l^-(r))^2 r^2 dr, \quad (\text{A.15})$$

$$G_{+-} = \int_0^\infty g_l^+(r)g_l^-(r)r^2 dr, \quad (\text{A.16})$$

$$F_{+-} = \int_0^\infty f_{l+2}^+(r)f_l^-(r)r^2 dr, \quad (\text{A.17})$$

$$F_{-+} = \int_0^\infty f_{l-2}^+(r)f_l^-(r)r^2 dr, \quad (\text{A.18})$$

$$F'_{-+} = \int_0^\infty f_l^+(r)f_{l+2}^-(r)r^2 dr. \quad (\text{A.19})$$

Apart from the case of G_+ , G_- , F_+ , F_- for $l = n - 1$, which are relatively easily obtained analytically, all other radial integrals have been calculated numerically (using quadruple precision).

The autocorrelation function can be calculated from (A.1) in a straightforward way:

$$\begin{aligned} \langle \Psi_r(0) | \Psi_r(t) \rangle = \sum_l \left\{ \exp(-iE_l^+ t) \left[\sum_m w_{l,m}^2 \left(a^2 \frac{l+1+m}{2l+1} + b^2 \frac{l+1-m}{2l+1} \right) \right] \right. \\ \left. + \exp(-iE_l^- t) \left[\sum_m w_{l,m}^2 \left(a^2 \frac{l-m}{2l+1} + b^2 \frac{l+m}{2l+1} \right) \right] \right\} \end{aligned} \quad (\text{A.20})$$

Appendix B.

Let us use the following notation:

$$k = j + 1/2, \quad \mathcal{E}_k = \frac{E_{nlj}}{m_0 c^2}, \quad x = (Z\alpha)^2. \quad (\text{B.1})$$

The exact eigenenergies \mathcal{E}_k (in units $m_0 c^2$) are given by

$$\mathcal{E}_k = \left[1 + \frac{x^2}{(n-k + \sqrt{k^2 - x^2})^2} \right]^{-1/2}. \quad (\text{B.2})$$

Expanding this expression in Taylor series with respect to x one obtains

$$\mathcal{E}_k = 1 - \frac{x^2}{2n^2} - \frac{x^4}{4n^3} \left(\frac{2}{k} - \frac{3}{2n} \right) - \frac{x^6}{4n^3} \left(\frac{1}{2k^3} + \frac{3}{2nk^2} - \frac{3}{n^2k} + \frac{5}{4n^3} \right) + [O(x)]^8. \quad (\text{B.3})$$

In eq. 7 only the lowest term depending on k in x^4 *i.e.* $\delta_4 \mathcal{E}_k = -\frac{x^4}{4n^3} \frac{2}{k}$ has been included. The higher order term $\delta_6 \mathcal{E}_k$ contributes very little, because the ratio $\delta_6 \mathcal{E}_k / \delta_4 \mathcal{E}_k = x^2 (\frac{1}{k^2} + \frac{3}{4nk} - \frac{3}{2n^2} + \frac{5k}{8n^3})$ reaches the maximum value about 0.0005 for $\epsilon = 0.4$ and $Z = 92$ and stays much smaller for lower Z . Then the time evolution for not too long period is mainly determined by the lowest order contribution (7).

The precession time is determined by the derivative

$$\frac{\partial \mathcal{E}_k}{\partial k} \Big|_{k=l_{av}} = \frac{x^4}{2n^3 k^2} \left[1 + \frac{3x^2}{2} \left(\frac{1}{2k^2} + \frac{1}{nk} - \frac{1}{2n^2} \right) \right]. \quad (\text{B.4})$$

Again in eqs. (8)-(9) only term of the order of x^4 has been used. The x^6 -order term contributes at most about 0.00022 of the x^4 -order term for $\epsilon = 0.4$ and $Z = 92$. Therefore we conclude that the x^6 -order term can be safely neglected in estimation of the precession time T_p .

References

- [1] For an introduction and a list of references see Schleich W P 2001 *Quantum Optics in Phase Space* (Berlin, Wiley-Vch.)
- [2] Bosanac S D 1993 *J. Phys. A: Math. Gen.* **25** 5523
- [3] Klystra N J, Ermolayev A M and Joachin C J 1997 *J. Phys. B: At. Mol. Opt. Phys.* **30** L449
- [4] Rathe U W, Keitel C H, Protopapas M and Knight P L 1997 *J. Phys. B: At. Mol. Opt. Phys.* **30** L531
- [5] Rutherford G H and Grobe R 1998 *J. Phys. A: Math. Gen.* **31** 9931
- [6] Su Q, Smetanko B A and Grobe R 1998 *Laser Phys.* **8** 93
- [7] Braun J W, Su Q and Grobe R 1999 *Phys. Rev. A* **59** 604
- [8] Wagner R E, Peverly P J, Su Q and Grobe R 1999 *Phys. Rev. A* **61** 035402
- [9] Krekora P, Wagner R E, Su Q and Grobe R 2001 *Phys. Rev. A* **63** 025404
- [10] Krekora P, Su Q and Grobe R 2001 *J. Phys. B: At. Mol. Opt. Phys.* **34** 2795
- [11] Nilsen H M, Masden L B and Hansen J P 2001 *J. Phys. B: At. Mol. Opt. Phys.* **34** L39
- [12] Arvieu R, Rozmej P and Turek M 2000 *Phys. Rev. A* **62** 022514
- [13] Arvieu R and Rozmej P 1994 *Phys. Rev. A* **50** 4376 ;
1996 *J. Phys. B: At. Mol. Opt. Phys.* **29** 1339
- [14] Averbukh I S and Perelman N F 1989 *Phys. Lett. A* **139** 449 ; 1989 *Sov. Phys. JETP* **69** 464
- [15] Rozmej P, Arvieu R, Averbukh I S and Turek M 2001 ECAMP VII, The Seventh European Conference on Atomic and Molecular Physics, Berlin, 2-6 April 2001, Europhysics Convergence Abstracts, Vol. 25B, p.99
- [16] Gay J C, Delande D and Bommier A 1989 *Phys. Rev. A* **39** 6587
- [17] Crawford M C 2001 *Am. J. Phys.* **69** 1182
- [18] Chang E C 1985 *Phys. Rev. A* **31** 495
- [19] Sommerfeld A 1921 *Atombau und Spektrallinien* (F. Fievag und Sohn, Braunschweig)
- [20] Rozmej P, Arvieu R 1999 *J. Phys. A: Math. Gen.* **32** 5637

This figure "F1_2.jpg" is available in "jpg" format from:

<http://arxiv.org/ps/quant-ph/0201015v2>

This figure "F3.jpg" is available in "jpg" format from:

<http://arxiv.org/ps/quant-ph/0201015v2>

This figure "F4.jpg" is available in "jpg" format from:

<http://arxiv.org/ps/quant-ph/0201015v2>

This figure "F5_6.jpg" is available in "jpg" format from:

<http://arxiv.org/ps/quant-ph/0201015v2>

This figure "F7_8.jpg" is available in "jpg" format from:

<http://arxiv.org/ps/quant-ph/0201015v2>

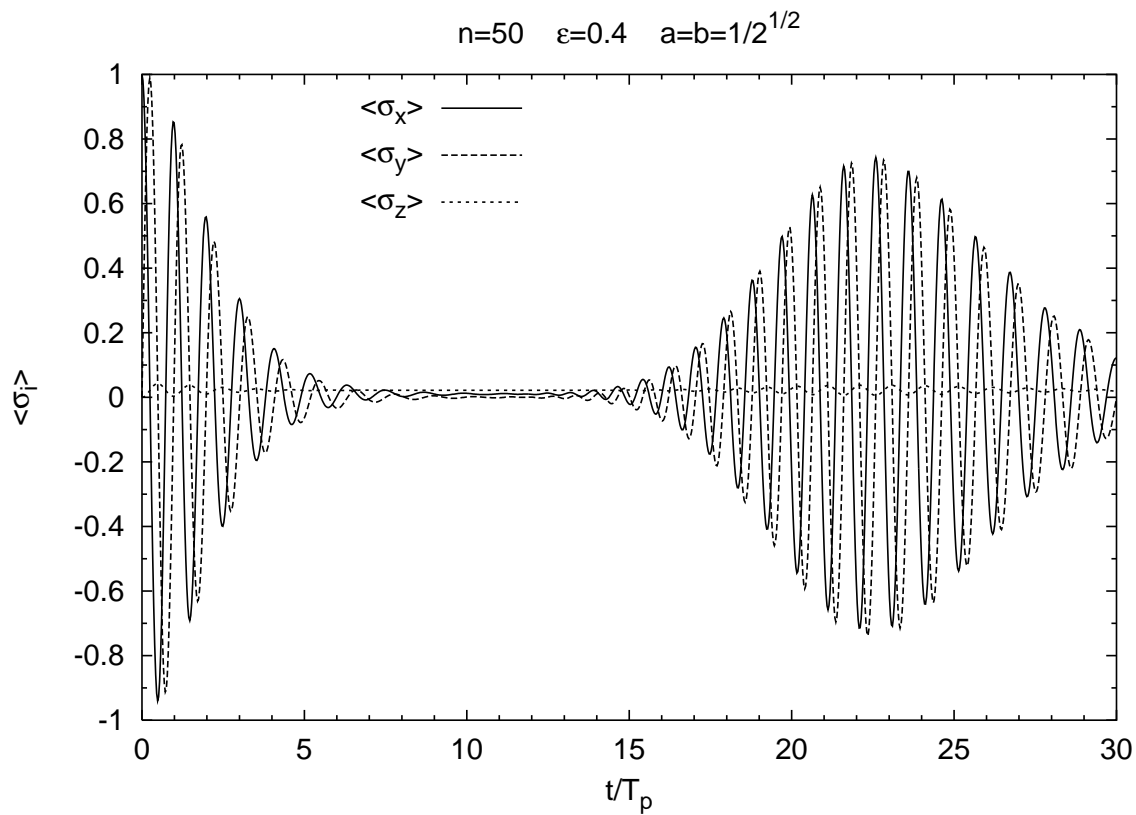


Figure 9. Time evolution of expectation values of spin components.